Application Note

Cell Migration and Invasion

Agilent

Trusted Answers

Automated Label-Free Cell Migration Assays Using Magnetic 3D Bioprinting

Authors

Brad Larson and Leonie Rieger
Agilent Technologies, Inc.
Winooski, VT, USA

Glauco R. Souza
Nano3D Biosciences, Inc.
Houston, TX, USA

Glauco R. Souza
The University of Texas Health Science Center at Houston
Houston, TX, USA

Abstract

Biocompatible magnetic particles and weak magnetic fields can be used to bioprint cells into aggregated structures that mimic tissues. A ring magnet was used to create keratinocyte rings for use in 3D wound healing experiments where cell migration into the interior of the ring was monitored. In addition, a spheroid magnet induced HCT116 cells into a spheroid shape suitable for a surrogate model for metastasis where both cells and extracellular matrix migrated away from the original spheroid structure. Both models used brightfield microscopy to quantify migration. Each migration can be inhibited by known cell migration inhibitors in a dose-dependent fashion suitable for pharmacological studies.

Introduction

Cell migration involves a cyclical coordinated procedure starting with cell polarization, protrusion, and substrate attachment of the leading edge, in addition to proteolytic degradation of physical barriers (e.g. tissue components and actinomyosin contraction) before the cell moves. Migration plays a central role in multiple beneficial physiological processes such as wound healing, in addition to being the first step in tumor metastasis as cells move away from the primary tumor site. Therefore, an advanced knowledge and methodology for monitoring phenotypic cell migration is useful for screening potential negative cytotoxic effects in test molecules, as well as speeding the development of novel therapies to reestablish wound healing abilities in pathologic tissue or control metastatic cellular invasion. Multiple techniques currently exist to assess cell migration. These commonly involve monitoring the migration of cells adhered to labware. The easiest and most sensitive of these methods incorporate label-free imaging to precisely track cell movement without introducing fluorescent probes that may affect normal cell activity. However, there are limitations to these migration assays. First, these assays use monolayers, which poorly mimic native tissue environments. In particular, these monolayers do not simulate tissue structure and properties, have altered cell exposure to compounds, and lack normal cell-cell and cell-extracellular matrix (ECM) interactions that characterize living tissue. Cell migration witnessed in monolayers may misrepresent behavior seen *in vivo*.

Three-dimensional (3D) cell culture platforms are potential solutions as they can reconstruct tissue structure and environments *in vitro*. In particular, incorporation of magnetic 3D bioprinting, where cells are magnetized and printed into appropriate 3D cell cultures, provides a method to reestablish missing interactions and easily create 3D phenotypic cell migration assays. Using this method, cells are magnetized with a biocompatible nanoparticle assembly consisting of gold, iron oxide, and poly-L-lysine that electrostatically and nonspecifically attaches to cell membranes. Magnetized cells are then directed using mild magnetic forces to form aggregates where cells interact and build larger 3D environments with ECM that represent native tissues. Cells and matrix can then be printed into different configurations to assess wound healing and metastatic cell movement. This application note presents two bioprinting procedures using different magnet geometries that enable *in vitro* 3D wound healing and metastatic cell migration experiments. Label-free cell migration using multiple skin and cancer cell models in 384-well format was tracked over time with automated widefield microscopy.

Materials and methods

Materials

Cells, assay, and experimental components

Immortalized keratinocytes (part number CRL-2309) and HCT116 colorectal carcinoma cells (part number CCL-247) were purchased from ATCC (Manassas, VA). The 384-well BiO assay kit (GBO part number 781846, consisting of 2 vials NanoShuttle-PL, 6-well levitating magnet drive, 384-well spheroid and holding magnet drives (2), 96-well deep well mixing plate, 6-well and 384-well clear cell repellent surface microplates), prototype 384-well ring drive, and additional cell-repellent surface 6-well (GBO part number 657860) and 384-well black µClear. microplates (GBO part number 781976), were generously donated by Nano3D Biosciences, Inc. (Houston, TX), and Greiner Bio-One, Inc., (Monroe, NC). Oridonin (part number O9639) was purchased from Sigma-Aldrich (St. Louis, MO). KU-0063794 (part number ENZ-CHM135) was generously donated by Enzo Life Sciences (Farmingdale, NY).

Agilent BioTek Cytation 5 cell imaging multimode reader

Cytation 5 is a modular multimode microplate reader combined with automated digital microscopy. Filter- and monochromator-based microplate reading are available, and the microscopy module provides up to 60x magnification in fluorescence, brightfield, color brightfield, and phase contrast. The instrument can perform fluorescence imaging in up to four channels in a single step. With special emphasis on live-cell assays, Cytation 5 features shaking, temperature control to 65 °C, CO_2/O_2 gas control, and dual injectors for kinetic assays, and is controlled by integrated Agilent BioTek Gen5 microplate reader and imager software, which also automates image capture, analysis, and processing. The instrument was used to kinetically monitor wound closure and cell migration activity using the brightfield channel.

Methods

3D cell preparation

Cells were prepared for magnetic bioprinting and levitation, including treatment with NanoShuttle-PL, according to the manufacturer's protocol (Figure 1). After preparation, cells were added to the 6-well cell-repellent plate, and a 6-well magnet was placed atop each well plate to levitate the cells, where they aggregated into 3D structures and induced ECM formation during a five-hour incubation at 37 °C/5% CO_2. After incubation, the cells and ECM were broken up, resuspended, and added to 384-well cell repellent plate wells.

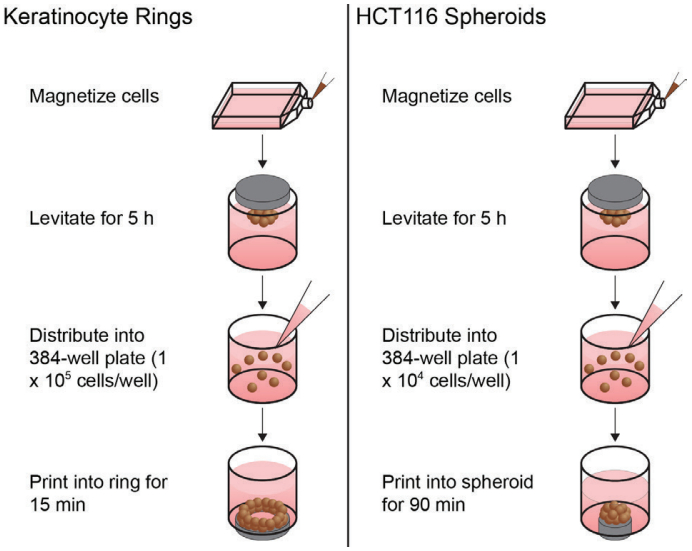

Figure 1. 384-well BiO assay kit protocol. 3D wound healing experiments used a ring magnet for bioprinting keratinocytes into ring structures (left side); whereas 3D spheroid cell migration experiments used a spheroid magnet for bioprinting HCT116 cells into spheroids (right side).

Wound healing assay protocol using ring magnet drive

Keratinocytes were added to the 384-well cell repellent plates at a concentration of 1.0×10^5 cells/well in a volume of 40 µL. A 384-well ring magnet was placed below the well plate, and the assembly was incubated at 37 °C/5% CO_2 for 15 minutes to allow cells to aggregate into the magnet's ring shape. Then, 10 µL of 5x concentrations of 200, 100, or 0 µM oridonin was added to the wells, and the plate was placed into the Cytation 5, preset to 37 °C/5% CO_2 where kinetic brightfield imaging, using a 4x objective, was performed every 30 minutes for 16 hours.

Cell migration assay protocol using spheroid magnet drive

HCT116 cells were added to the 384-well cell-repellent plates at a concentration of 1.0×10^4 cells/well in a volume of 40 µL. A 384-well spheroid magnet was placed below the well plate, and the assembly was incubated at 37 °C/5% CO_2 for 90 minutes to allow cells to aggregate into a spheroid. Then, 10 µL of 5x concentrations of KU-0063794, ranging from 50,000 to 0 nM were added to the wells, and the plate was placed into Cytation 5, preset to 37 °C/5% CO_2 where kinetic brightfield imaging, using a 2.5x objective, was performed every 15 minutes for 48 hours.

Results and discussion

Label-free image-based 3D wound healing monitoring

The ability of the 3D-bioprinted ring structure to demonstrate wound healing, and the capability of automated image-based monitoring and analysis was initially examined. As shown in Figures 2A and 2B, the untreated keratinocyte 3D ring structure contracted over time, while oridonin had an inhibitory effect on wound closure (Figures 2C and 2D). This also demonstrated the ability of Cytation 5 to track 3D cellular movement throughout the entire incubation period.

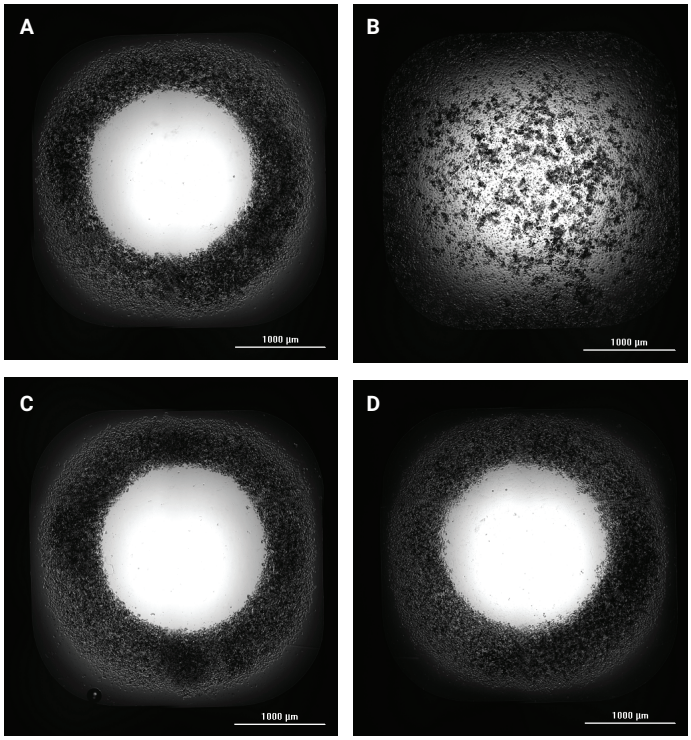

Figure 2. Wound healing using 3D-bioprinted keratinocyte ring structures. Stitched brightfield images of 3 row by 2 column montage tiles, using a 4x objective, treated as follows: (A) 0 µM oridonin, 0 hours incubation; (B) 0 µM oridonin, 16 hours incubation; (C) 40 µM oridonin, 0 hours incubation; (D) 40 µM oridonin, 16 hours incubation.

Original brightfield images were then preprocessed (Figure 3A) to smooth the background signal and remove the halo effect seen in brightfield imaging (Figure 3B). An image plug was then placed on each image of appropriate size to always include a portion of the ring structure. Upon placement, cellular analysis was conducted using parameters such that the contrast between signal from the bioprinted ring area and background (Figure 3C) was used to place accurate object masks around the portion of the cellular area within each mask (Figure 3D). Use of preprocessed images improved the accuracy of object mask placement. Through use of this analysis procedure, the total cell and ECM area within the plug at time 0 and throughout the incubation period could be tracked.

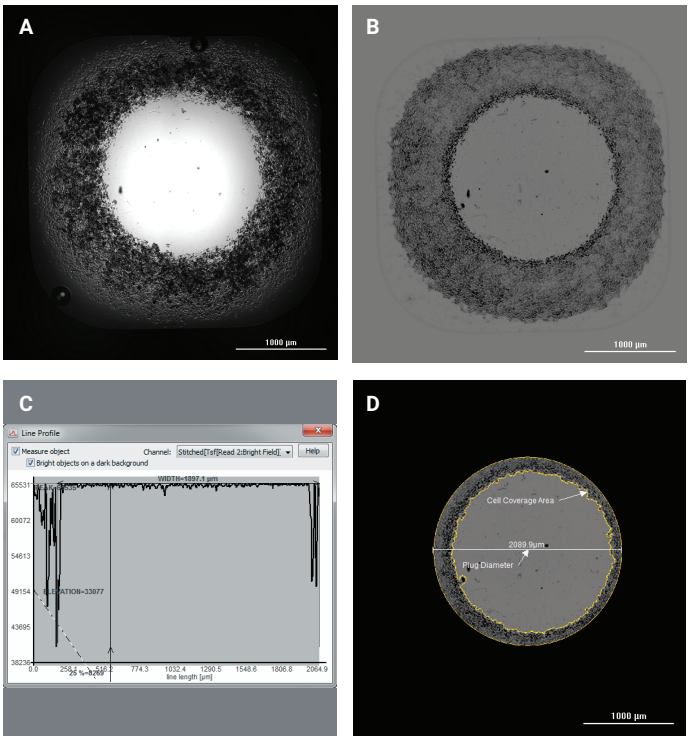

Figure 3. Agilent BioTek Gen5 cellular analysis of 3D wound healing images. Representative (A) unprocessed, and (B) preprocessed brightfield image, captured using a 4x objective and 3 × 2 image montage. (C) Graph of brightfield signal across the diameter of the image plug through areas containing cells and noncellular areas. (D) Representative cellular analysis image showing plug diameter and object mask placement around the cellular area within the plug.

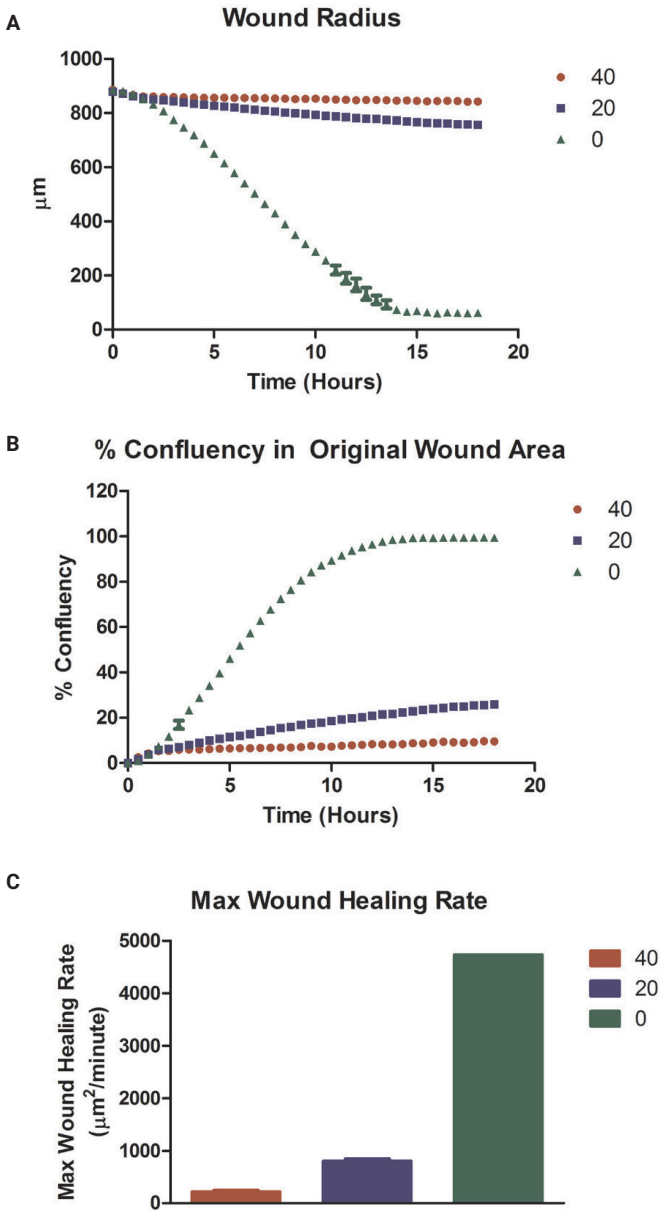

Figure 4. Calculated kinetic 3D wound healing graphs. Graphs of (A) wound radius, (B) % cell confluency in the original wound, and (C) maximum wound healing rate plotted for vehicle, 20 and 40 µM oridonin.

The Gen5 calculated metric of Sum Area$_t$ (total cellular area within the plug) was used to quantify multiple metrics of cell migration as a function of time in the kinetic assay. Wound radius was the radius of the circular area uncovered by cells within each image plug. Percent confluency in the original wound area was the area of cells and ECM migrating into the original calculated wound area, expressed as a percentage, and maximum wound healing rate was the highest rate of slope increase, or V_{max}, from the kinetic % confluency in the original wound graphs. Each metric was also automatically calculated by Gen5 and used to determine the uninhibited healing rate of test cell types, or the ability of molecules to modify initial rates of wound healing.

For experiments conducted in this study, the keratinocyte/ECM combination migrated at a rate where complete wound closure was seen within 14 hours. Migration was then modified by oridonin, so that near complete inhibition could be achieved using a 40 µM concentration. These findings confirm the ability of the 3D image-based assay procedure for use with wound healing applications.

Label-free 3D cell migration monitoring

Detection and quantification of metastatic cell migration was then examined using a similar 3D bioprinting and image-based analysis procedure. Brightfield images were captured of HCT116 cells and ECM migrating away from the original bioprinted area over the incubation period (Figure 5A). Image preprocessing was again performed to remove the dark areas of the image, allowing easier visualization of the leading edges of the migrating structure which have a minimal change in contrast with the image background (Figure 5B). HCT116 cell migration could then be visualized (Figures 5C and 5D), as well as interruption of cell movement by 10 µM concentrations of the known inhibitor KU-0063794 (Figures 5E and 5F).

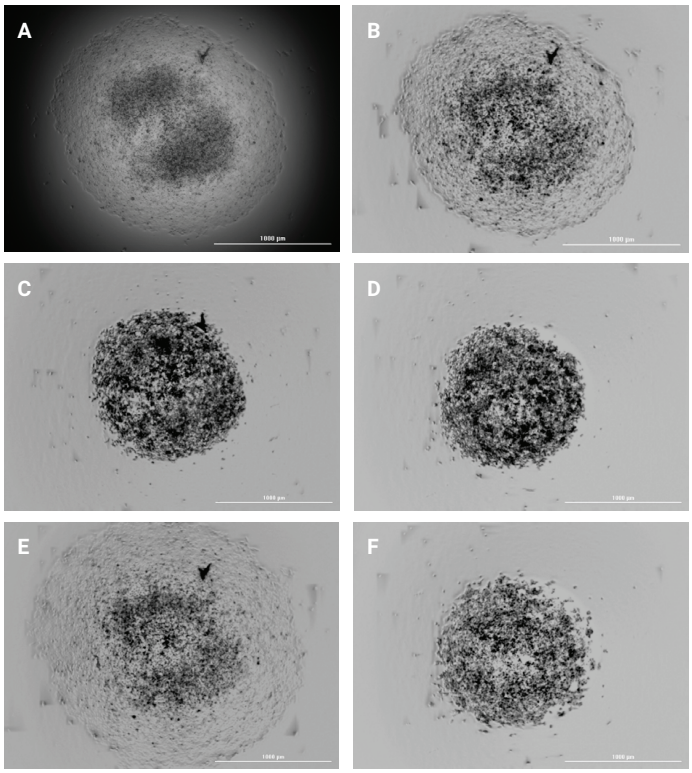

Figure 5. Cell and ECM migration in 3D-bioprinted HCT116 cells and ECM. (A) Unprocessed and (B) preprocessed brightfield images captured using a 2.5x objective. Preprocessed images of 3D-printed cells treated as follows: (C) untreated, 0 hours incubation; (D) untreated, 48 hours incubation; (E) 10 µM KU-0063794, 0 hours incubation; (F) 10 µM KU-0063794, 48 hours incubation.

Using Gen5 software, object masks were placed around the migrating structure, once again using the changes in brightfield signal between areas of the image containing cells and ECM and noncellular background areas (Figure 6A). The process allowed detailed object mask placement (Figure 6B), and accurate tracking of cell movement.

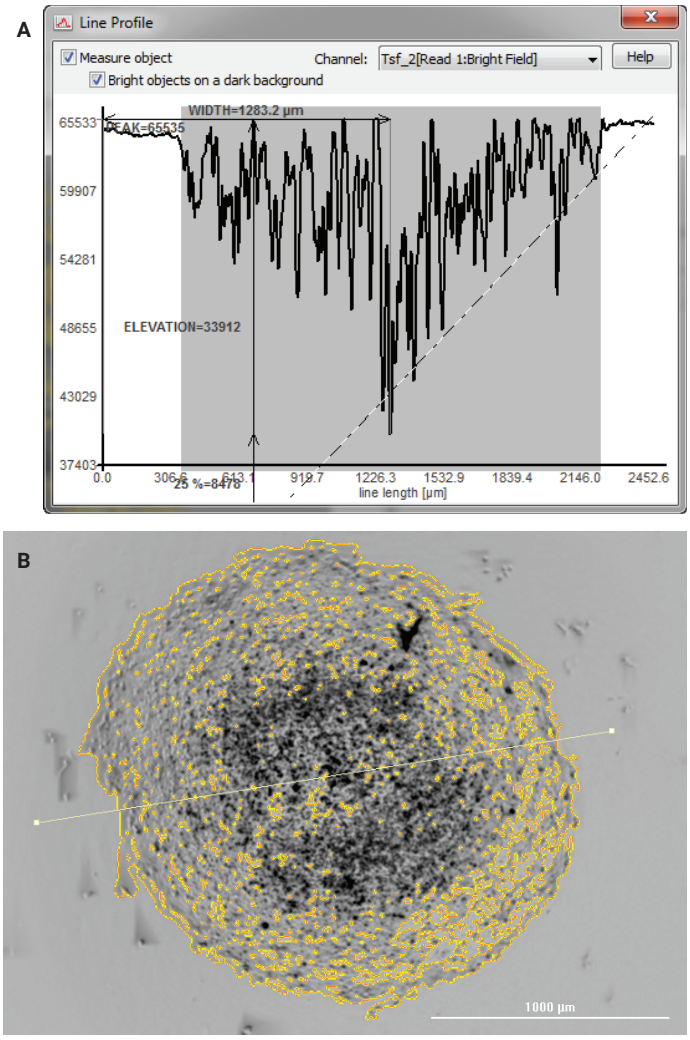

Figure 6. Agilent BioTek Gen5 object mask placement on preprocessed brightfield images. Representative brightfield image, using a 2.5x objective. (A) Line analysis showing change in brightfield intensity from the middle of the 3D spheroid to the edge; (B) object masks automatically placed around cells using Gen5 software.

Area within each object mask was automatically returned by Gen5 as a calculated metric at each time point for the KU-0063794 concentrations tested. Coverage area values, along with fold change values calculated by comparing object areas at each time point to those from time 0, were then graphed (Figure 7).

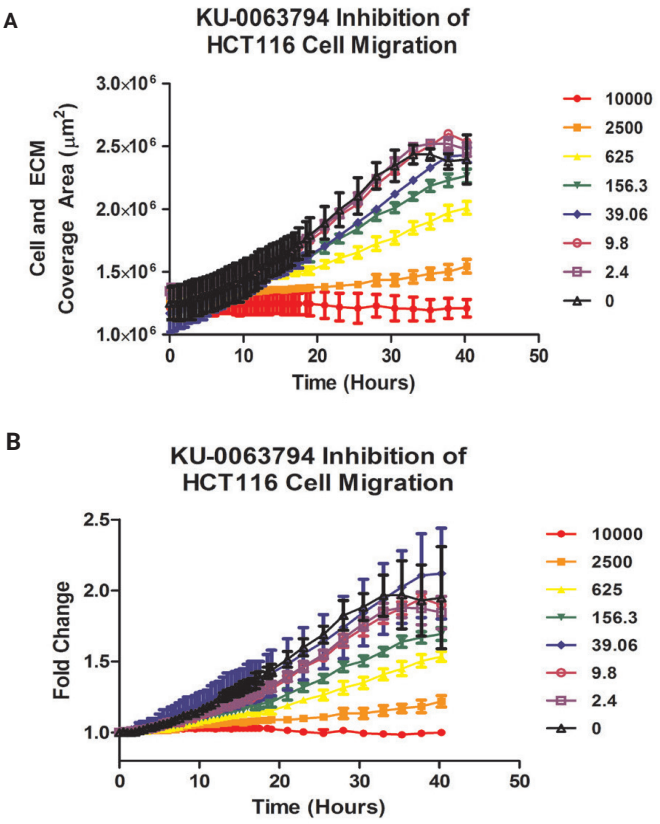

Figure 7. Kinetic HCT116 cell migration analysis. (A) Coverage area of cells exposed to 0 to 10,000 nM KU-0063794. (B) KU-0063794 area fold change calculations compared to coverage area at time 0.

The results in Figure 7 demonstrate that KU-0063794 has a dose-dependent effect on HCT116 cell and ECM movement, and further validates the use of the 3D bioprinting and image-based process to assess metastatic cell migration.

Area under the curve was then calculated using the change in cell area coverage values from the kinetic dose-response curves seen in Figure 7A. Four different time points were chosen (10, 20, 30, and 40 hours), and area under the curve for each concentration tested was plotted. From the generated curve fits, IC_{50} values were calculated (Figure 8). Upon examination of the curves and IC_{50} values, it can be seen that the concentration of KU-0063794 required to inhibit cell movement increases as the incubation period also increases, illustrating the advantage of performing kinetic monitoring of cell migration as opposed to imaging at only one end point.

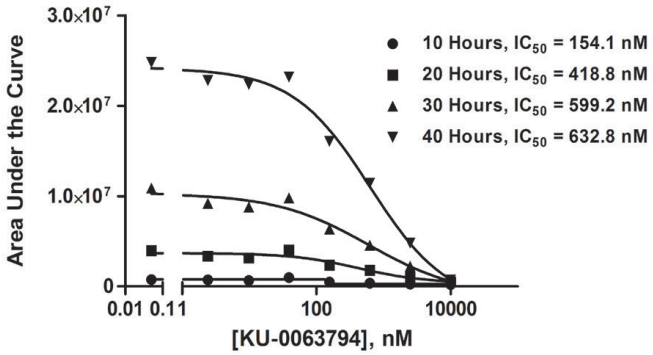

Figure 8. Area under the curve (AUC) and IC_{50} values for cells treated with KU-0063794 at varying time intervals.

Conclusion

The 384-well BiO assay kit and NanoShuttle-PL particles from n3D Biosciences provide a simple, high-throughput method to carry out biomimetic, 3D determinations of wound healing and metastatic cell migration. Additionally, the automated imaging capabilities of Agilent BioTek Cytation 5 cell imaging multimode reader simplify the experimental process by allowing label-free tracking of cell/ECM movement. Performing kinetic imaging also provides the advantage of assessing the effect of test molecules at multiple time points. Advanced cellular analysis tools in Agilent BioTek Gen5 microplate reader and imager software allow accurate and detailed analysis, with all data generated by a single instrument. The combination of assay method and automated imaging and analysis creates a robust, high-throughput method to generate *in vivo*-like assessments of 3D cell movement.

www.agilent.com/lifesciences/biotek

RA44412.4

Printed in the USA, April 8, 2022
5994-3383EN

Agilent
Trusted Answers